Precise interplanetary network localization of the bursting pulsar GRO J1744-28

Hurley, K.; Kouveliotou, C.; Cline, T.; Cole, D.; Miller, M.C.; Harmon, A.; Fishman, G.J.; Briggs, M.; van Paradijs, J.A.; Kommers, J.; Lewin, W.H.G.

Published in:
Astrophysical Journal

DOI:
10.1086/309083

THE ASTROPHYSICAL JOURNAL, 537:953–957, 2000 July 10

PRECISE INTERPLANETARY NETWORK LOCALIZATION OF THE BURSTING PULSAR GRO J1744−28

K. HURLEY
University of California, Berkeley, Space Sciences Laboratory, Berkeley, CA 94720-7450
C. KOUVELIOTOU
Universities Space Research Association, NASA Marshall Space Flight Center, ES-84, Huntsville, AL 35812
T. CLINE
NASA Goddard Space Flight Center, Greenbelt, MD 20771
D. COLE
Jet Propulsion Laboratory, MS 169-327, Pasadena, CA 91109
M. C. MILLER
University of Maryland, Department of Astronomy, College Park, MD 20742-2421
A. HARMON AND G. FISHMAN
NASA Marshall Space Flight Center, ES-84, Huntsville, AL 35812
M. BRIGGS
University of Alabama in Huntsville, AL 35899
J. VAN PARADIJS[1,2]
University of Alabama in Huntsville, AL 35899
AND
J. KOMMERS AND W. LEWIN
Massachusetts Institute of Technology, Center for Space Research 37-627, Cambridge, MA 02139
Received 1999 December 23; accepted 2000 February 11

ABSTRACT

We analyze 426 observations of the bursting pulsar GRO J1744−28 by *Ulysses* and BATSE. Triangulating each burst and statistically combining the triangulation annuli, we obtain a 3 σ error ellipse whose area is 532 arcsec^2. The accuracy of this statistical method has been independently verified with observations of the soft gamma repeater SGR 1900+14. The ellipse is fully contained within the 1′ radius *ASCA* error circle of the soft X-ray counterpart and partially overlaps the 10″ radius *ROSAT* error circle of a source which may also be the soft X-ray counterpart. A variable source which has been proposed as a possible IR counterpart lies at the edge of the 3 σ error ellipse, making it unlikely from a purely statistical point of view to be associated with the bursting pulsar.

Subject headings: pulsars: individual (GRO J1744−28) — stars: neutron — X-rays: stars

1. INTRODUCTION

The bursting pulsar GRO J1744−28 was discovered with the Burst and Transient Source Experiment (BATSE) aboard the *Compton Gamma-Ray Observatory* (*CGRO*) in 1995 December (Fishman et al. 1995; Kouveliotou et al. 1996a). Between the discovery date and 1997 April, BATSE detected over 5800 type II bursts (i.e., accretion-powered; Lewin et al. 1996) from this source (Woods et al. 1999), many of which were also detected by instruments aboard the *Rossi X-Ray Timing Explorer* (*RXTE*: Giles et al. 1996) and *Ulysses* among others (e.g., Konus-WIND: Aptekar et al. 1998). The initial source localization was a 6° radius error circle (Fishman et al. 1995). Triangulation with BATSE and *Ulysses* resulted in a 24′ wide annulus which intersected this error circle, and the use of the BATSE Earth occultation technique reduced the area of the localization further (Hurley et al. 1995). Observations using the Oriented Scintillation Spectrometer Experiment (Kurfess et al. 1995; Strickman et al. 1996) and BATSE observations of a variable, pulsating (467 ms period) quiescent source associated with the bursting source (Finger et al. 1996a, 1996b; Paciesas et al. 1996) resulted in a still smaller error box. A subsequent *RXTE* observation produced an $\approx$5 arcmin^2 error box (Swank 1996; Giles et al. 1996). Within this error box, Frail et al. (1996a, 1996b) found a variable radio source. Observations of the region around the radio source position with the *Advanced Satellite for Cosmology and Astrophysics* (*ASCA*) revealed a pulsating, bursting X-ray source with the same 467 ms period (Dotani et al. 1996a, 1996b) whose position was consistent with that of the radio source, but a later *ROSAT* observation (Kouveliotou et al. 1996b; Augusteijn et al. 1997) with higher angular resolution found an X-ray source within the 1′ radius *ASCA* error circle which was significantly displaced from the radio position. The radius of the *ROSAT* error circle is 10″, corresponding to a 5″ statistical error and a 8″ systematic error, summed in quadrature. No confidence level can be quoted for the systematic error, but the statistical error corresponds to $\sim$10 σ (J. Greiner 1999, private communication).

Although the radio source was rejected as a possible counterpart to GRO J1744−28, optical and near-infrared observations of the *ROSAT* source region did uncover an object at the limit of the 10″ radius *ROSAT* error circle which appeared to be variable (Augusteijn et al. 1997; Cole et al. 1997). These observations were carried out at the European Southern Observatory (ESO) and at the Astrophysical Research Consortium's Apache Point Observatory

[1] Astronomical Institute "Anton Pannekoek," University of Amsterdam, The Netherlands.
[2] Deceased.

(APO). In some of the observations, it was not possible to rule out the apparent detection as an instrumental artifact (Augusteijn et al. 1997); in others, however, there was no reason to suspect that the detection was not valid (Cole et al. 1997).

It has been proposed that GRO J1744−28 is a low-mass X-ray binary system (LMXB), in which a neutron star with a dipole field $B \lesssim 10^{11}$ G accretes matter from its companion. The rotation period of the neutron star is 467 ms, the orbital period of the system is 11.8 days, and the system is viewed nearly face-on (e.g., Daumerie et al. 1996). The distance is approximately that of the Galactic center.

Because of the difficulty of identifying the counterpart at various wavelengths in a crowded region of the sky toward the Galactic center, it is important to consider the details of the *ROSAT* observation. It was a short one (820 s) with the High Resolution Imager (HRI); only 273 photons were collected, and, in contrast to the *ASCA* observation, neither pulsations nor bursts were detected. (During the observation, no bursts were recorded by BATSE or *Ulysses* either, and the upper limit to the *ROSAT* pulsed flux is consistent with that derived from BATSE and *RXTE* observations.) From earlier *ROSAT* observations in which the source was not detected, it was concluded that the object was transient; based on the statistics of transient sources in the Galactic plane, it was estimated that the probability of observing a random source unrelated to the bursting pulsar was less than 10^{-4}. Since no energy spectra are recorded by the HRI, the *ASCA* spectrum was assumed to calculate the source flux; it was found to be $\approx 2 \times 10^{-9}$ ergs cm^{-2} s^{-1} (unabsorbed) in the 0.1–2.4 keV energy range (Augusteijn et al. 1997). This observation took place in 1996 March. For comparison, the fluxes measured by *ASCA* in the 2–10 keV energy range were 2×10^{-8} ergs cm^{-2} s^{-1} in 1996 February and 5×10^{-9} ergs cm^{-2} s^{-1} in 1997 March (Nishiuchi et al. 1999). These fluxes would convert to unabsorbed 0.1–2.4 keV fluxes of 9.7×10^{-9} ergs cm^{-2} s^{-1} and 2.4×10^{-9} ergs cm^{-2} s^{-1}, respectively, using a simple extrapolation of the power-law continuum measured by Nishiuchi et al. (1999).

To summarize, there are good arguments both in favor of and against the idea that the true X-ray and optical/IR counterparts to GRO J1744−28 have been identified. In favor:

1. This was the only *ROSAT* source detected within the *ASCA* error circle,
2. It was transient, and
3. The variable optical/IR source was reliably detected in some of the observations of Cole et al. (1997).

Against:

1. No bursts or pulsations were observed by *ROSAT* (although the short duration of the observation may be to blame);
2. Augusteijn et al. (1997) estimate that the proposed optical/IR counterpart, if real, exhibited a change in its IR flux by a factor of 10 over a period of minutes, with no accompanying X-radiation; the detection could have been an artifact; and
3. The proposed optical/IR counterpart lies at the edge of or just outside the *ROSAT* error circle (depending on the astrometry).

Here we adopt the view that the true counterpart to GRO J1744−28 may not yet have been identified and localized with certainty, and we analyze the observations of bursts from GRO J1744−28 by *Ulysses* and BATSE in order to better constrain the position of the source.

2. OBSERVATIONS

We began this analysis by examining *Ulysses* gamma-ray burst (GRB) experiment (Hurley et al. 1992) data for each BATSE burst. Knowing the arrival time of a burst at BATSE, the coordinates of the *Ulysses* spacecraft, and the approximate source position, we extracted data for $\sim \pm 100$ s about the *Ulysses* crossing time. Although the bursting pulsar was a prolific source, it was not a particularly intense one, and this procedure resulted in the identification of only ≈ 500 bursts in the *Ulysses* data. Typically, these were count rate increases in the 3–6 σ range. The vast majority of them were recorded in the untriggered data, which have a time resolution of 0.25–2 s, depending on the telemetry mode. We then retained only those bursts which were recorded by BATSE with 0.064 s time resolution, since these are the ones which can be cross-correlated with the *Ulysses* time histories with the best accuracy. Figure 1 shows one example. The final data set then consisted of 426 bursts, of which only five were recorded by *Ulysses* in triggered (32 ms resolution) data. The first event in this set was BATSE 4042 on 1995 December 19, and the last was BATSE 6085 on 1997 February 2.

Triangulation of a single burst results in an annulus of possible arrival directions whose width depends on the vector between the two spacecraft and the uncertainty in cross-correlating the two time histories (see, e.g., Hurley et al. 1999a). As examples, we show the first and last annuli in Figure 2. Their widths are $\approx 0\overset{\circ}{.}9$ and $3\overset{\circ}{.}8$ (1 σ), respectively, and they intersect at an angle $\approx 37^\circ$, approximately the same angle as the displacement of the Earth-*Ulysses* vector during the period between the bursts. In Figure 3 we show

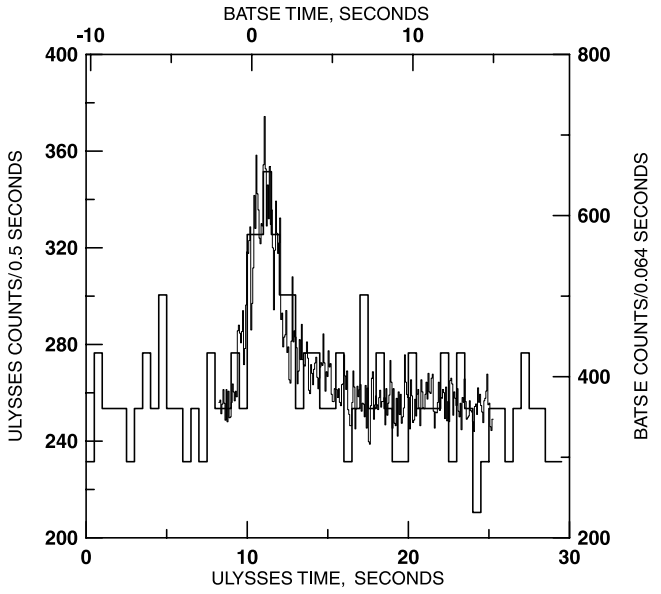

FIG. 1.—*Ulysses* (thick line) and BATSE (thin line) time histories for trigger 4317. The *Ulysses* time resolution is 0.5 s, and the data are for the 25–150 keV energy range. The BATSE time resolution is 0.064 s, and the data are for the 25–100 keV energy range. The time histories are aligned for the best-fitting lag.

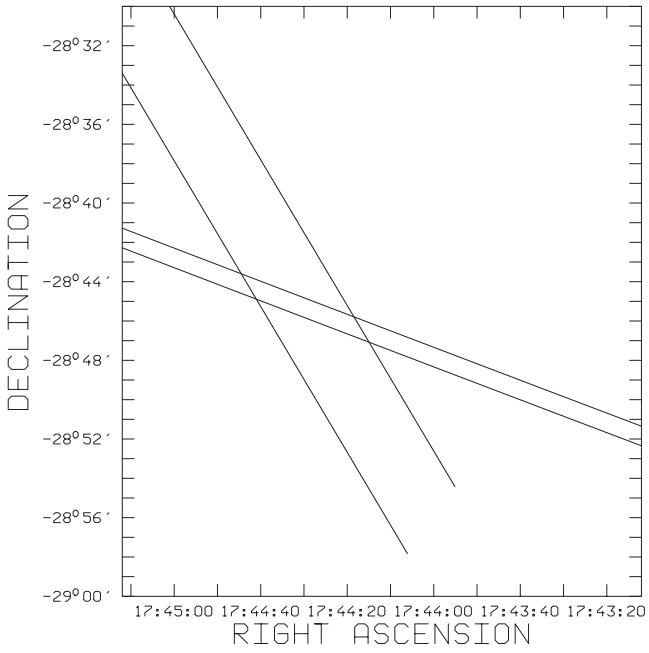

FIG. 2.—Triangulation annuli for the first and last bursts in this study. The first annulus, for BATSE 4042 on 1995 December 19, is the narrower one; its width is $\approx 0.'9$ (1 σ). The last annulus is for BATSE 6085 on 1997 February 2; its width is $3.'8$ (1 σ).

the distribution of the 426 annulus half-widths. The average total width is $\approx 3.'2$. We can predict what the approximate result might be of combining these annuli statistically. Two $3.'2$ wide annuli intersecting at an angle of 37° form a box shaped roughly like a rhombus with diagonals $3.'4$ and $10'$. (The actual error region will be an ellipse inscribed in the rhombus, with minor and major axes somewhat smaller than the diagonals; for the purposes of this simple estimate we ignore this fact and base our calculation on the lengths of the diagonals, which will give us an overestimate of the final error region size.) The statistical combination of the 426 annuli should therefore be an elliptical error region with minor and major axes approximately $3.'4/\sqrt{426}$ and $10'/\sqrt{426}$, or $10''$ and $29''$, respectively. We show below that these are in fact close to, but larger than, the final dimensions.

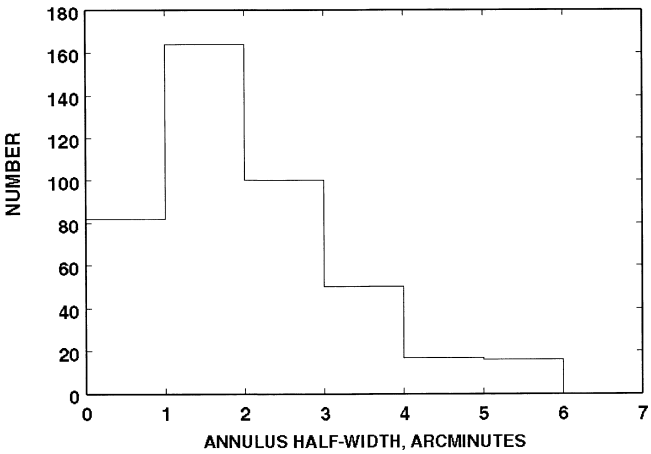

FIG. 3.—The distribution of the 426 annulus half-widths. The average is $\approx 1.'6$.

The statistical method for combining the results of multiple triangulations has been outlined in Hurley et al. (1999b). It consists of defining a χ^2-distributed variate which is a function of an assumed source position in right ascension and declination, and of the parameters describing the triangulation annuli. Let α, δ be the right ascension and declination of the assumed source position, and let α_i, δ_i, θ_i be the right ascension, declination, and radius of the ith annulus. Then the angular distance d_i between the two is given by

$$d_i = \theta_i - \cos^{-1} [\sin \delta \sin \delta_i + \cos \delta \cos \delta_i \cos (\alpha - \alpha_i)] . \quad (1)$$

If the 1 σ uncertainty in the annulus width is σ_i, then

$$\chi^2 = \sum_i \frac{d_i^2}{\sigma_i^2} . \quad (2)$$

The assumed source position is varied to obtain a minimum χ^2; 1, 2, and 3 σ equivalent confidence contours in α and δ are found by increasing $\chi^2_{\rm min}$ by 2.3, 6.2, and 11.8.

The best-fitting position for the 426 annuli is $\alpha(2000) = 17^{\rm h}44^{\rm m}32^{\rm s}$, $\delta(2000) = -28°44'31.''7$ and has a $\chi^2_{\rm min}$ of 415.7 for 424 degrees of freedom (426 annuli, minus the two fitting parameters α, δ). For a large number of degrees of freedom m, the χ^2 distribution approaches the normal distribution with standard deviation $\sqrt{2m}$ and mean m. Thus the value we obtain for χ^2 lies 0.27 standard deviations from the mean and is an acceptable fit. Figure 4 shows the best-fitting position, the *ROSAT* error circle, a portion of the *ASCA* error circle, and the two slightly different positions for the proposed optical counterpart found by Augusteijn et al. (1997) and Cole et al. (1997) (these sources are likely to be one and the same, considering their quoted astrometric uncertainties), along with the 1, 2, and 3 σ error ellipses obtained in this analysis. The Augusteijn et al. (1997) and the Cole et al. (1997) positions for the proposed counterpart lie at $\chi^2_{\rm min} + 12.3$ and $\chi^2_{\rm min} + 15.3$, or at the

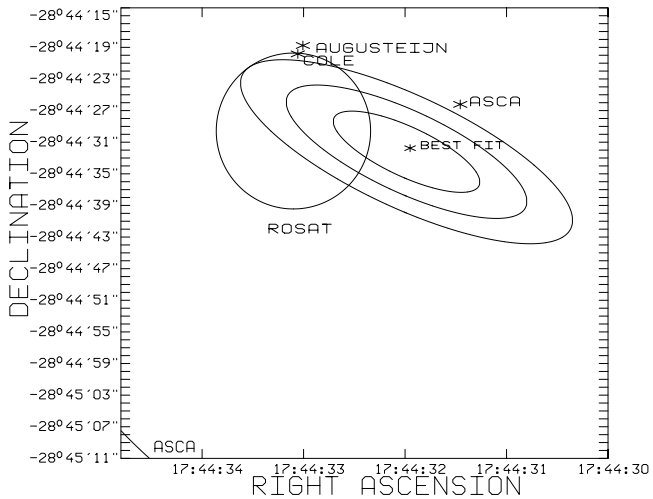

FIG. 4.—An $\sim 1' \times 1'$ square region containing the best-fitting position for the statistical combination of the 426 annuli. The 1, 2, and 3 σ error ellipses surround this position. The $10''$ radius *ROSAT* error circle is also shown. The center of the $1'$ *ASCA* error circle is marked; part of the circle is visible in the lower left hand corner. The two slightly different positions for the proposed optical counterpart found by Augusteijn et al. (1997) and Cole et al. (1997) are indicated.

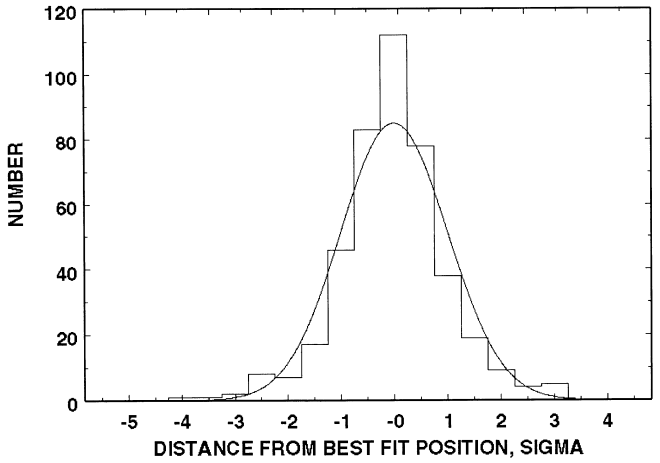

FIG. 5.—The distribution of the minimum distances between the 426 annuli and the best-fit position α_{bf}, δ_{bf}. The minimum distance for annulus i is given by $d_i = \theta_i - \cos^{-1}$ [sin δ_{bf} sin δ_i + cos δ_{bf} cos δ_i cos $(\alpha_{bf} - \alpha_i)$], where α_i, δ_i, and θ_i are the right ascension, declination, and radius of the ith annulus. The distances have been normalized to the annulus widths σ_i. For comparison, a Gaussian is plotted with mean zero, standard deviation unity, normalized to the area under the histogram.

99.8% and 99.95% confidence levels, respectively. The VLA source position is off the map; it lies at $\chi^2_{min} + 1709$, and is definitely excluded as a candidate in this analysis. The parameters of the 1, 2, and 3 σ error ellipses are given in Table 1. Figure 5 shows the distribution of the distances between the individual annuli and the best-fit position.

3. ACCURACY OF THE METHOD

One of the design goals of the *Ulysses* mission was an absolute timing accuracy of several milliseconds. To confirm that no large errors exist in the spacecraft timing and ephemeris, end-to-end timing tests are routinely carried out, in which commands are sent to the GRB experiment at precisely known times, and the times of their execution on board the spacecraft are recorded and compared with the expected times. Because of command buffering on the spacecraft, there are random delays in the execution of these commands, and the timing is verified to different accuracies during different tests. The tests just before, during, and just after the series of 426 bursts analyzed here took place on 1995 December 5, 1996 October 1, and 1997 February 19 and indicated that the timing errors at those times could not have exceeded 50, 3, and 1 ms, respectively. For comparison, the 1 σ uncertainties in these triangulations are all greater than 125 ms. This includes both the statistical errors and a conservative estimate of possible unknown timing and spacecraft ephemeris errors.

Two other independent confirmations of the accuracy of the triangulation method are first, the excellent agreement between the VLA and triangulated positions of SGR 1900+14, using the same statistical method as the one we employ here (Hurley et al. 1999b); and second, the agreement between the triangulated positions and the positions of gamma-ray bursts with optical and/or X-ray counterparts (e.g., Hurley et al. 2000).

TABLE 1

PARAMETERS OF THE 1, 2, AND 3 σ ERROR ELLIPSES

Ellipse	Minor Axis (arcsec)	Major Axis (arcsec)	Area (arcsec^2)
1 σ.....	6.4	20.7	104
2 σ.....	10.5	34.0	279
3 σ.....	14.4	46.9	532

Although there is no reason to suspect timing errors, it is difficult to prove beyond a doubt that they do not exist, so we have investigated the effects which such errors would have. We distinguish between two hypothetical types. The first is a constant, systematic offset in the timing of one spacecraft. For example, if the difference in the burst arrival times at the two spacecraft were systematically overestimated by a constant value of the order of several hundred milliseconds for each burst, the result would be to increase the radii of all the annuli, leaving the annulus widths and the coordinates of the annulus centers unchanged. (The increase in each radius would be almost, but not exactly, the same, since it depends on the value of the interspacecraft vector, which changes from burst to burst as the spacecraft move.) The new annuli would still be consistent with a best-fitting position with an acceptable χ^2_{min}, but the position would shift by 15″ for every 100 ms of offset.

The second is a random error whose average value is zero, but whose value for any given burst may take on positive or negative values up to several hundred milliseconds. To simulate the effects of such errors we have added a random number to the difference in the spacecraft arrival times for each burst; the number is drawn from a Gaussian distribution with mean zero and standard deviation 100 ms. The effect of such an error would again be to change only the radii of all the annuli, but by different amounts whose average would be zero. Since the annulus widths are unaffected, the χ^2_{min} for the best-fitting position increases, but not to the point where it becomes unacceptable or even suspect. The best-fitting position shifted by 6″ in this simulation.

Other types of errors can of course be imagined, but we reiterate that there is neither any indication that such errors exist nor any means to disprove their existence entirely.

4. DISCUSSION AND CONCLUSIONS

Because pulsations and bursts were detected during the *ASCA* observation, there is no doubt that *ASCA* detected the X-ray counterpart to GRO J1744−28, but it is not well localized. If we accept the *ROSAT* source as the counterpart, then the combination of the 3 σ error ellipse derived here and the *ROSAT* error circle gives a new, smaller error box whose area is $\approx$150 arcsec^2, or about one half the *ROSAT* area. One reason to accept it is the fact that the error ellipse indeed overlaps it partially; we estimate the chance probability of an overlap between the two within the *ASCA* error circle to be $\sim$0.14. If we reject the *ROSAT* source as the counterpart, the appropriate error box for GRO J1744−28 becomes the entire 532 arcsec^2 3 σ error ellipse. However, this implies that the X-ray counterpart must have faded to an undetectable flux during the *ROSAT* observation, or $< 5 \times 10^{-12}$ ergs cm^{-2} s^{-1} (unabsorbed).

In either case, the possible variable IR source is at or beyond the 3 σ confidence levels of both the *ROSAT* and the triangulation regions. From a purely statistical point of view it is unlikely to be the counterpart, but it cannot be completely ruled out. The Interplanetary Network (IPN) error ellipse has been examined in four of the archived K' images taken at APO and ESO. Their dates and limiting magnitudes are 1996 January 21 (APO: 14.4 $\pm$ 0.3), 1996

January 30 (APO: 15.2 ± 0.3), 1996 February 8 (ESO: 16.75 ± 0.3), and 1996 May 1996 (ESO: 17.1 ± 0.3). Comparing the first three with the last reveals no variable objects other than the previously identified IR source. However, based on the magnitudes of LMXBs, Augusteijn et al. (1997) estimated that the quiescent counterpart to GRO J1744−28 might have a K magnitude ≈ 18.7, or at least two magnitudes fainter than the completeness limit of their observations, and Cole et al. (1997) estimated that observations down to $K' = 20$ were needed. It is also possible that the true counterpart is considerably farther away than the Galactic center, or that absorption in this direction is greater than expected.

Fortunately, it may be possible to resolve the ambiguity. The X-ray counterpart can be detected in an observation with the *Chandra* High Resolution Camera (HRC) if its flux has not decreased by more than a few orders of magnitude. Detection of pulsations would lead to an unambiguous identification of the counterpart, and the subarcsecond HRC resolution would provide the smaller error box needed to carry out deeper searches for the IR counterpart.

K. H. is grateful to JPL for *Ulysses* support under contract 958056 and to NASA for Compton Gamma-Ray Observatory support under grant NAG 5-3811.

REFERENCES

Aptekar, R., et al. 1998, ApJ, 493, 404
Augusteijn, T., et al. 1997, ApJ, 486, 1013
Cole, D., et al. 1997, ApJ, 480, 377
Daumerie, P., Kolgera, V., Lamb, F., & Psaltis, D. 1996, Nature, 382, 141
Dotani, T., Ueda, Y., Ishida, M., Nagase, F., Inoue, H., & Saitoh, Y. 1996a, IAU Circ. 6337
Dotani, T., Ueda, Y., Nagase, F., Inoue, H., & Kouveliotou, C. 1996b, IAU Circ. 6368
Finger, M., Koh, D., Nelson, R., Prince, T., Vaughan, B., & Wilson, R. 1996b, Nature, 381, 291
Finger, M., Wilson, R., Harmon, B., Hagedon, K., & Prince, T. 1996a, IAU Circ. 6285
Fishman, G., Kouveliotou, C., van Paradijs, J., Harmon, B., Paciesas, W., Briggs, M., Kommers, J., & Lewin, W. 1995, IAU Circ. 6272
Frail, D., Kouveliotou, C., van Paradijs, J., & Rutledge, R. 1996a, IAU Circ. 6307
———. 1996b, IAU Circ. 6323
Giles, A., Swank, J., Jahoda, K., Zhang, W., Strohmayer, T., Stark, M., & Morgan, E. 1996, ApJ, 469, L25
Hurley, K., Briggs, M., Kippen, R., Kouveliotou, C., Meegan, C., Fishman, G., Cline, T., & Boer, M. 1999a, ApJS, 120, 399
Hurley, K., Kouveliotou, C., Cline, T., Mazets, E., Golenetskii, S., Frederiks, D., & van Paradijs, J. 1999b, ApJ, 523, L37
Hurley, K., Kouveliotou, C., Harmon, A., Fishman, G., Briggs, M., van Paradijs, J., Kommers, J., & Lewin, W. 1995, IAU Circ. 6275
Hurley, K., et al. 2000, ApJ, 534, 258
Hurley, K., et al. 1992, A&AS, 92, 401
Kouveliotou, C., Greiner, J., van Paradijs, J., Fishman, G., Lewin, W., Rutledge, R., Kommers, J., & Briggs, M. 1996b, IAU Circ., 6369, 1
Kouveliotou, C., van Paradijs, J., Fishman, G., Briggs, M., Kommers, J., Harmon, B., Meegan, C., & Lewin, W. 1996a, Nature, 379, 799
Kurfess, J., Grove, J., & Tueller, J. 1995, IAU Circ. 6276
Lewin, W., Rutledge, R., Kommers, J., van Paradijs, J., & Kouveliotou, C., 1996, ApJ, 462, L39
Nishiuchi, M., et al. 1999, ApJ, 517, 436
Paciesas, W., Harmon, B., Fishman, G., Zhang, S., & Robinson, C. 1996, IAU Circ. 6284
Strickman, M., et al. 1996, ApJ, 464, L131
Swank, J. 1996, IAU Circ. 6291
Woods, P., et al. 1999, ApJ, 517, 431